Experimental Heat Transfer, vol. 3, pp. 447–463, 1990

VISUALIZATION OF NUCLEATE FLOW BOILING FOR AN R22/R114 MIXTURE AND ITS COMPONENTS

M. A. Kedzierski and D. A. Didion
National Institute of Standards and Technology, Thermal Machinery Group, Gaithersburg, Maryland 29899

Visualization of bubble nucleation during forced-convective flow inside a horizontal, electrically heated quartz tube was done in order to establish a comparison of this phenomenon between refrigerant mixtures and their pure components. The specific phenomena investigated were the suppression of nucleation due to increased mass flow quality while holding all other conditions fixed, and the comparison of the nucleate activity of the binary mixture to the nucleate activity of the pure components. The fluids investigated were a 37.7 mol% R22/62.3 mol% R114 binary mixture and the individual components R22 and R114. These fluids were pumped through an abraded, electrically heated quartz tube. A 16-mm high-speed camera was used, at 7000 frames/s, to film the boiling process. Detailed measurements of bubble frequency and bubble size were possible at low pressures, allowing direct calculation of the latent heat load required to nucleate a single bubble. Further work is required to develop a method that ensures statistically sound bubble frequency measurements. However, the standard deviations of the bubble diameter measurements were acceptable. The films were used to visually demonstrate the suppression of nucleation with increase in quality for R114, R22, and an R22/R114 mixture. The films suggest that, for a given quality, R114 exhibits much more nucleation than either R22 or the mixture, while the amount of nucleation demonstrated by R22 and the mixture was comparable even though the mixture was mostly R114 by mole. Arguments using the latent heat of vaporization, the vapor density, and the liquid thermal conductivity have been made to explain the visual trends.

INTRODUCTION

Investigators have found that phase change by means of bubble nucleation is more efficient for a single liquid component than it is for a mixture of two or more liquids [1–3]. Heat transfer coefficients for pool boiling of multicomponent mixtures, where the growth of bubbles at a solid–liquid interface is the main heat transfer mechanism, are in general lower than those of the individual components [3]. Depending on the quality, both bubble nucleation and interface evaporation can be important in the boiling of a flowing fluid within a horizontal tube. Jung [4] has found that heat transfer coefficients for flow boiling of refrigerant mixtures inside horizontal tubes are characteristically lower than those that would be obtained from an ideal mixing rule between the pure components (and sometimes even lower than either component). His study revealed that

This work was funded jointly by NIST and EPRI RP 8006-2 under project manager Jong Kim. The authors would like to thank Dong Soo Jung, Michael Kauffeld, and Mark McLinden for their valuable inputs toward the completion of this work.

of the refrigerant as compared to that of water, but this cannot be known for certain without further investigation.

There is not sufficient understanding of nucleate boiling of multicomponent mixtures to develop a model to predict such a phenomenon. The criterion most commonly used to determine if suppression has occurred is to examine the heat transfer data for lack of heat flux dependence. Although this seems to be based on sound rationale, there still exists a large degree of uncertainty since this criteria is derived from pressure, temperature, and mass flow measurements, not from visual observation. The nucleate boiling contribution to total heat transfer is obtained by subtracting what is thought to be the convective portion from the total. Thus, both the nucleate boiling and the convective boiling portions are obtained by indirect measurement.

This article presents a case study of nucleate flow boiling. The results presented here are by no means useful in the design of evaporators. That is, neither heat transfer coefficients nor wall superheats are presented. Instead, visual results that characterize the mechanisms of nucleate flow boiling are presented. It is intended that the characterization of the boiling will stimulate thought on the measurement and the cause of the fundamental mechanisms that govern the heat transfer. The first objective of this study is to become familiar with the difficulties associated with obtaining detailed bubble measurements and what is required to overcome these problems. Three sections of this article deal with situations encountered and remedies revealed in the experimental logic, and measurements methods. The second objective of this study is to visually demonstrate the suppression of nucleate boiling with increasing quality for flow boiling within a horizontal tube. The visual demonstration of suppression is useful because it verifies that suppression does occur and because the relationship between suppression and quality can be experimentally quantified. Future studies may establish a comparison between suppression for refrigerants and other fluids, e.g., water. The third objective is to compare the relative activity of nucleate flow boiling for an R22/R114 mixture of arbitrary composition to that for the single components R22 and R114 for the same heat flux and flow conditions. The resulting data have been used to demonstrate the relative differences between bubble generation in binary mixtures and that in single-component refrigerants. Also, the data can be used to determine if the bubble activity of the flowing mixtures is degraded in a similar magnitude as for mixtures in pool boiling experiments.

TEST APPARATUS

Figure 1 shows a schematic of the visualization test section. The 9-mm-ID quartz tube was enclosed in a housing as shown. The space between the inside of the housing and the outside of the tube was filled with glycerol to limit reflections from the tube, which would have otherwise caused poor photographic images. A 16-mm high-speed camera was used to make motion-picture films of the flow boiling process within the horizontal quartz tube. The camera was positioned in front of the sight glass so that the plane of the view was parallel to the direction of flow. Figure 1 also shows that a 500-W concentrated light source was placed in front of another sight glass opposite the camera to produce a back-lighting configuration. An opaque cover was placed between the light and the sight glass to give uniform illumination of the quartz tube. The inside of the quartz tube was polished with a 5-μm abrasive to create a surface similar to the

inside of stainless steel tubing. Similarity of the quartz roughness to the steel roughness was verified by visual inspection with an electron microscope. The roughened surface would ensure active cavity nucleation. The quartz tube was electrically heated by a 4-mm-wide copper strip placed along the bottom of the outside of the tube. The localized heat flux produced nucleation only at the bottom of the tube. Bubble growth on the sides and top of the tube was not present, which ensured an unobstructed view of the bubble growth on the tube bottom.

The main test rig is shown in Fig. 2. This test rig was used by Jung in his work. A more detailed discussion of it can be found in his thesis [4]. The main test rig was used to set the mass flow rate and the entering quality to the visualization section. Figure 2 shows that the test rig consists of two 4-m lengths of 9.1-mm-ID, 0.25-mm-wall thickness 304 stainless steel tube connected by a U-bend. The tubing was heated by a DC voltage which produced a constant-heat-flux boundary condition. The test fluid was pumped through the inside of the tube and increased in quality as it boiled along the length until it reached the condenser, where it was condensed and returned to the pump. Measured tube wall temperatures and fluid pressures of the main test rig were used to calculate the quality at the entrance to the visualization section. A detailed discussion of the calculation of the quality is given in a later section.

Figure 2 shows that a 2-m calming section was used to connect the visualization test section to the main test rig. This length is not electrically heated, but it receives a marginal amount of heat from the surroundings (not enough to cause nucleation). The calming section allows most of the remaining bubbles from the main test rig to combine with the main vapor slug so that these bubbles will not be attributed as being generated in the quartz tube. This ensures that only those bubbles generated in the quartz tube will be photographed and analyzed.

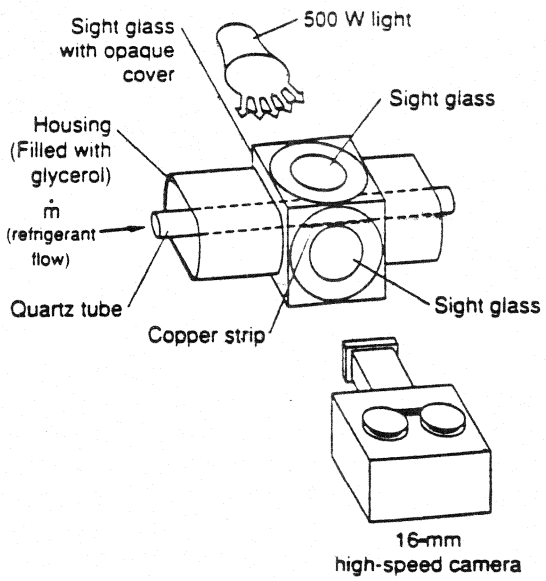

Fig. 1 Schematic of the visualization test section.

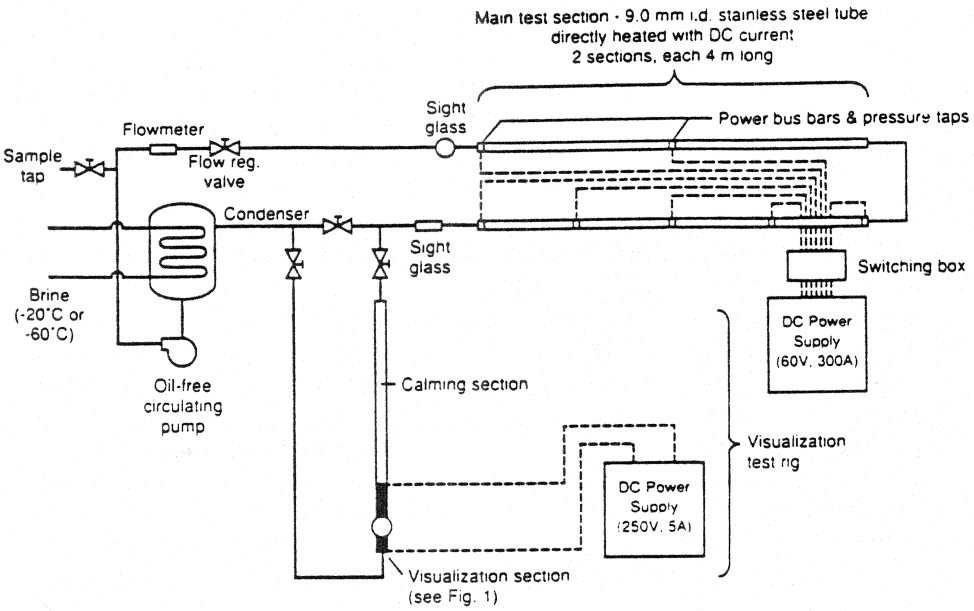

Fig. 2 Main test rig and visualization section.

EXPERIMENTAL LOGIC

This section outlines the logic used to choose the thermodynamic conditions at which the tests were conducted. The final operating condition was dictated by the lower temperature limit of the test rig.

The first step was to choose the operating parameters which would be fixed while varying quality and fluid. From examination of correlations [1, 4–6], it was felt that the refrigerant total mass flow rate ($\dot{m}$) and the heat flux (q) to the quartz tube were strong functions of heat transfer and should be held constant for all tests. The authors also felt that the remaining operating condition to be chosen as fixed was the fluid pressure. Cooper [7] has shown that, for most fluids, nucleate boiling on the outside of horizontal cylinders is proportional to the following form involving only reduced pressure (P_r):

$$\frac{h}{(q/A)^{0.69}} \propto P_r^{0.056}(-\log_{10} P_r)^{-0.7} \tag{1}$$

Equation (1) shows that the heat transfer by nucleation has the same functional form regardless of the fluid. Thus the magnitude of nucleate boiling for different fluids should differ only by a constant. Consequently, as Eq. (1) suggests, comparisons of the data for the different fluids were made at equal P_r. The next step was to determine the P_r at which to operate the tests.

Two criteria were used to choose the pressure at which the tests were conducted. First, the pressure had to be below the structural limitations of the test rig. Second, in order to make direct measurements of bubble growth, it was essential that an unobstructed view of the bubble be attained. Equation (1) implies that nucleate boiling measurements taken at low reduced pressure will have fewer active sites. Individual bubbles

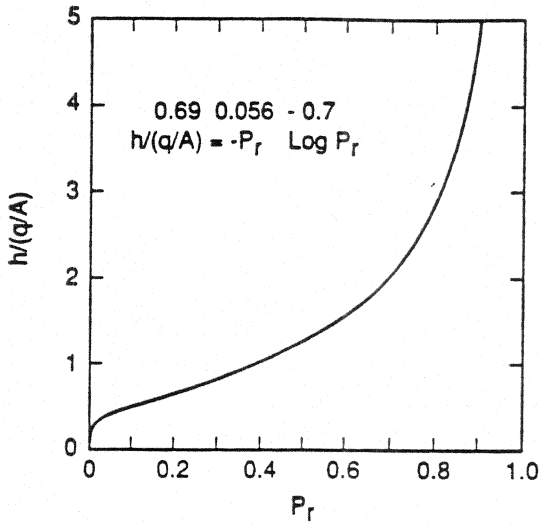

Fig. 3 Functional form of pool boiling data given by Cooper [7].

are less likely to be disturbed by other bubbles for low-P_r boiling, since there is less interaction between bubbles. Thus it was possible to examine a single bubble and measure directly the bubble diameter and frequency for R114 data at $P_r = 0.015$. After consideration of the structural limitations and the desired visual conditions, a low reduced pressure was chosen for test. The final step was to determine the magnitude of P_r for test.

Figure 3 is a plot of the right side of Eq. (1) versus P_r. Figure 3 shows that the nucleate boiling potential increases sharply with P_r for $P_r < 0.05$ and for $P_r > 0.8$, and is comparatively flat for $0.05 < P_r < 0.8$. This demonstrates that measurements taken in the region $0.05 < P_r < 0.8$ would be less sensitive to the inaccuracies of the pressure measurement. However, preliminary tests with R114 showed that the number of active sites present for $0.05 < P_r < 0.8$ prohibited examination of the growth of a single bubble. The tests were finally conducted at the lowest possible P_r which was attainable in the test rig, which was $P_r = 0.015$ for R114. At this pressure, examination of individual bubble growth was possible for R114.

Attempts were made to take data for all fluids at $P_r = 0.015$. Unfortunately, the lowest temperature limit of the existing test rig was not sufficient to attain $P_r = 0.015$ for R22 and the mixture. The lowest possible P_r attainable in the test rig for R22 and the mixture was $P_r = 0.063$. The consequence of taking data at $P_r = 0.063$ can be examined with the aid of Eq. (1). Figure 3 shows that there is a 62% increase in the nucleate boiling potential from $P_r = 0.015$ to $P_r = 0.063$. The investigators found that indeed there were many more bubbles present at $P_r = 0.063$ than there were at $P_r = 0.015$ for R114. Detailed measurement of bubble parameters was not possible at $P_r = 0.063$ due to the frequent interaction of bubbles. As a result, the data at high P_r was analyzed subjectively. Because the data sets were analyzed differently, the experimental results were discussed separately as high- and low-P_r conditions. Refrigerants 22, 114, and the mixture were all examined at $P_r = 0.063$, which is referred to here as the high-P_r condition. Only R114 was examined at $P_r = 0.015$ (low P_r).

EXPERIMENTAL MEASUREMENTS

The bubble frequency and the bubble size can both be measured at low reduced pressures. The bubble frequency, f_b, was obtained by counting the number of motion-picture frames (N) from the growth to the release of the bubble from the solid–liquid interface and dividing by the steady-state film speed (S); i.e.,

$$f_b = \frac{S}{N} \tag{2}$$

Care was taken to ensure that measurements were made only when the film speed had reached 7000 frames/s. Timing marks on the film were used for this purpose. The bubble departure diameter (D_b) was the maximum diameter of the bubble obtained just after departure from the wall–liquid interface. The bubble diameter was obtained by measuring both the bubble diameter and the quartz tube diameter from the film and scaling down to obtain D_b from the known quartz tube diameter. The bubble geometry was approximated as spherical for the calculation of the amount of vapor contained in the bubble. Efforts were made to measure the bubble size soon after departure from the wall and also when it appeared to be most spherical. The volume of vapor generated for a single bubble per unit time (V_b) was calculated as

$$V_b = \frac{f_b \pi D_b^3}{6} \tag{3}$$

From V_b, the latent portion of the heat load required to generate one bubble (Q_b) is

$$Q_b = \lambda \rho_v V_b \tag{4}$$

The accuracy of the calculation for Q_b is not calculable. The calculation relies on the ability to quantify the deviation of the bubble shape from spherical. If the uncertainty in the shape of the bubble can be represented as an error in the measurement of D_b, then a 10% error in the measurement of D_b will cause a 30% error in the calculation of V_b and, consequently, a 30% error in the calculation of Q_b. Although the accuracy of Q_b is unknown, it is felt that since the experimental procedure was consistent for all the data, the Q_b can be used successfully to investigate trends.

High-pressure data (P_r = 0.06–0.065) at a mass flow rate of 0.032 kg/s and a quartz tube heat flux of 64 kW/m^2 was taken for R22, R114, and the R22/R114 mixture. At this pressure, individual bubbles could not be isolated for study due to vigorous interaction with other bubbles. The temperature of the brine that was supplied to the condenser of the main test rig was not low enough to operate at lower pressures for R22 and the mixture. Consequently, the comparison of bubble nucleation for the different liquids remains mostly visual and subjective.

CALCULATION OF MASS QUALITY

This section discusses the procedure used to calculate the quality (x) at the entrance to the visualization test section. Mass quality (x) is defined as the fraction of the

total mass flow which is vapor:

$$x = \frac{\dot{m}_v}{\dot{m}} = \frac{Q}{\dot{m}\lambda} \tag{5}$$

The total mass flow rate ($\dot{m}$) is measured at the subcooled entrance to the main test rig with a calibrated turbine meter. The latent heat of vaporization (λ) is obtained from an equation of state for refrigerants and refrigerant mixtures derived by Morrison and McLinden [8]. The heat available for boiling (Q) is a sum of that which is obtained from electrical heating in the main test rig (Q_p) and obtained from the surroundings (Q_∞) minus the heat required to bring the entering subcooled liquid to saturation (Q_s); i.e.,

$$Q = Q_p + Q_\infty - Q_s \tag{6}$$

The Q_∞ is obtained from a calibrated UA and measured temperature difference between the room and the average fluid temperature for the 2-m calming section. The Q_s was calculated as $\dot{m}C_p(T_s - T_i)$, where T_s is the saturation temperature of the refrigerant and T_i is the temperature of the subcooled liquid entering the main test rig.

The gain in temperature due to viscous heating was calculated to be less than 0.1 K for all tests. The calculated qualities below 5% have an uncertainty of approximately ±12% for 99.7% confidence. The quality calculations in the range 9–20% quality have an uncertainty of approximately ±5% for 99.7% confidence.

A visual method for calculating the quality using a photographic estimate of the void fraction and calculated density was also conducted. The uncertainty of the visual method was approximately only ±20%. Consequently, this method was used only as a check on the calculation of the quality given by Eqs. (5) and (6). The quality calculated from Eqs. (5) and (6) was within the scatter of the quality obtained by the visual method.

EXPERIMENTAL RESULTS

Pure R114 at $P_r = 0.015$

The following is a discussion of the experimental results of the convective nucleate boiling of R114 at $P_r = 0.015$. Measurements of f_b and D_b were done only for pure R114.

Figure 4 shows photographs taken from the high-speed films for R114 at $P_r = 0.015$. The film number and the refrigerant number are located on the upper tube wall of the photographs. The dark area along the bottom of the quartz tube is the copper strip used to heat the fluid electrically. The main liquid–vapor interface of the flow is the dark, wavy line approximately one-third of a tube diameter up from the tube bottom. The vapor slug is above the liquid–vapor interface, and the liquid film is below the liquid–vapor interface. The vapor slug was surrounded by liquid for all qualities. The vapor bubbles are shown to be within the liquid and carried from the wall from left to right of the photograph.

Figure 4 shows that approximately 10 different sites were visible along the 15-mm quartz tube length. Not all sites were present for all qualities. For example, the majority

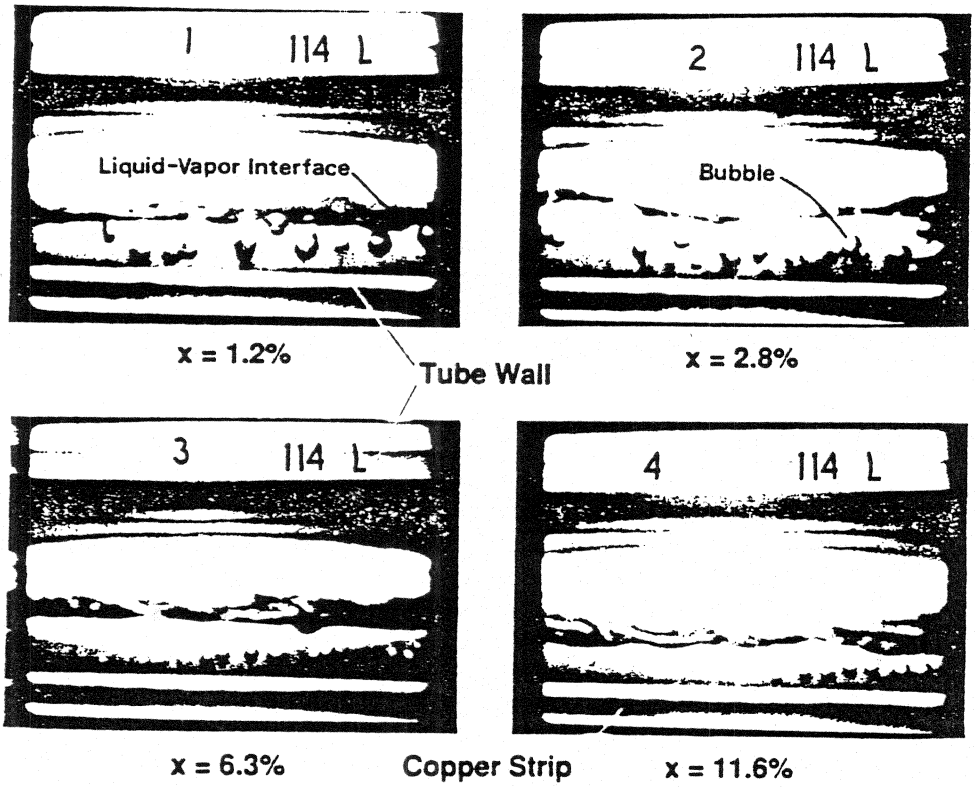

Fig. 4 Flow boiling of R114 at $P_r = 0.015$.

of sites were active at the lowest quality ($x = 0.012$), and only one site was active at the highest quality ($x = 0.116$), clearly demonstrating suppression of bubble growth at increased quality. However, some sites that were active at, say, $x = 0.063$ were not active at $x = 0.012$. Hence these sites are not sufficient to demonstrate suppression due to quality increase. Only two sites were active for all qualities except the highest quality. Consequently, only the data of these two sites for R114 at $P_r = 0.015$ are discussed in the following. The authors feel that the f_b and D_b of the reported two sites measured at a given quality are representative of the f_b and D_b observed at the same quality for sites not reported.

Figure 5 shows the variation of the measured bubble frequency (f_b) with quality (x) for two different nucleation sites, indicated by filled and open circles. The f_b was obtained by averaging the frequency of five consecutive bubbles originating from the same site. One standard deviation for the measurement trials was approximately 16% of the measurement and is represented as an error bar for a data point of Fig. 5. The large standard deviations are due to local changes in the flow conditions, which are characteristic of chaotic flows. It is difficult to extract a functional relationship from data with such a large standard deviation, which is compounded by a small change in the average f_b with quality. Consequently, no generalizations about the variation of f_b can safely be made. It is possible that the bubble frequency is coupled with quality and the wall temperature profile, which is continually disturbed by the growth and release of adjacent

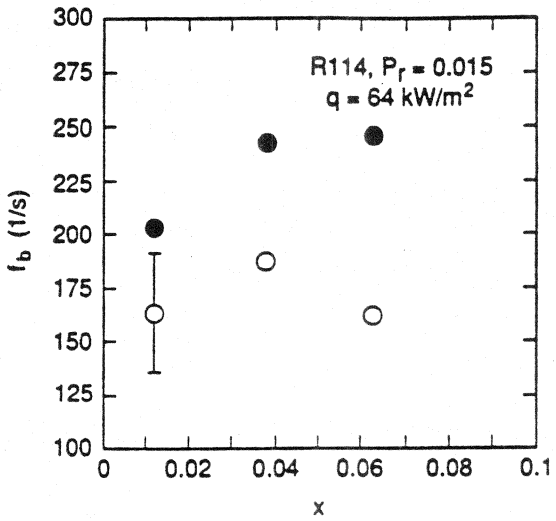

Fig. 5 Measured bubble frequency for different qualities.

bubbles. Clearly, more work must be done toward establishing a measurement method for f_b that will produce statistically sound data.

Figure 6 is a plot of the measured bubble diameter (D_b) versus quality. The standard deviation of the measured bubble diameter is relatively small, and the change of D_b with quality is significant. Hence the plot clearly suggests a relatively linear relation between decreasing bubble diameter and increasing quality. This is not to say that this relation is appropriate for all boiling surfaces, fluids, and flow conditions. The purpose here is merely to suggest that measurement of the bubble diameter on high-speed film can produce successful results.

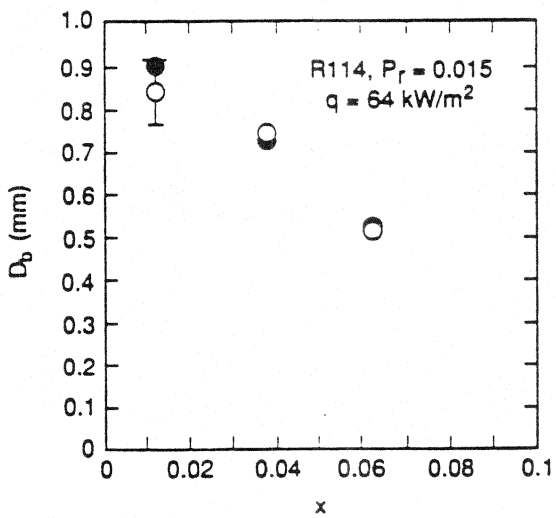

Fig. 6 Measured bubble diameter for different qualities.

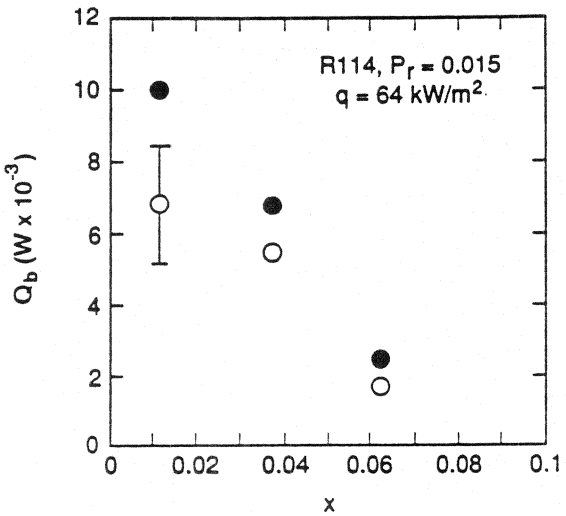

Fig. 7 Heat load required to nucleate one bubble continuously for a particular quality.

The heat imposed with the electrically heated copper strip (Q_e) onto the bottom of the quartz tube is dissipated by two very different mechanisms. The first mechanism is nucleate boiling. Nucleate boiling requires a superheated liquid layer and sites from which bubbles can grow. The focus of measurements in this article is on the latent component of nucleate boiling (Q_b), i.e., only the heat for phase change and not the energy for superheating the liquid. The heat that is not used to nucleate is conducted and convected through the liquid film to the liquid–vapor interface, where it is convected and evaporated away by the vapor phase. This second mechanism is called convective evapo-

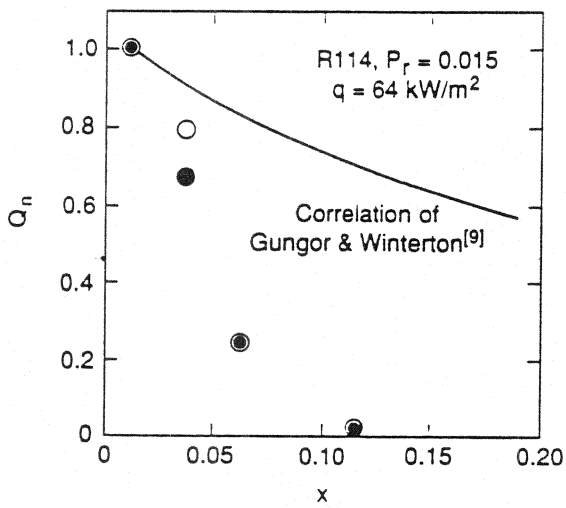

Fig. 8 Comparison of measured heat load to theory of Gungor and Winterton [9].

ration (Q_c) in this article. The first resistance to convective evaporation is the liquid film on the tube wall. Low thermally conductive liquids (like refrigerants), thick films (low qualities), and small velocities (low mass flow rates) all contribute to the resistance to Q_c. The resistance to Q_c decreases for increasing quality due to smaller liquid film thickness and higher liquid and vapor velocities associated with high qualities. Consequently, the fraction of Q_e which is Q_c increases for increasing quality. The fraction of Q_e which is Q_b correspondingly decreases for increasing quality.

Equation (4) was used along with the measured f_b and D_b to calculate the heat load required to generate one vapor bubble (Q_b) and plotted versus quality in Fig. 7. Figure 7 demonstrates, as discussed above, that Q_b decreases with increasing quality for fixed

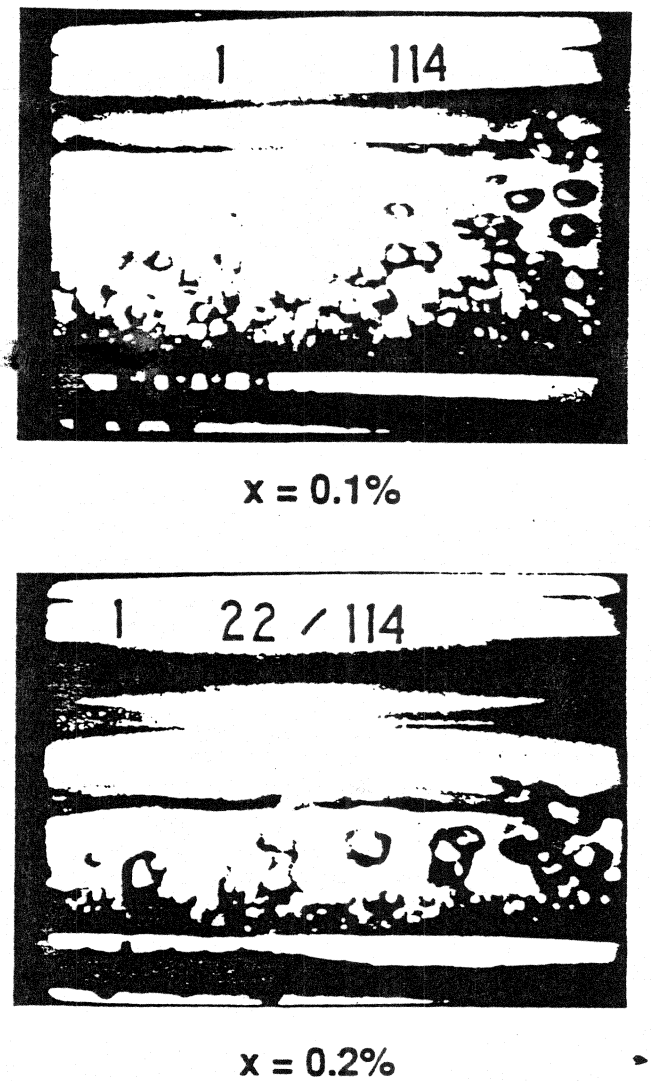

Fig. 9 Flow boiling for R114 and a mixture for x = 0.1%. P_r = 0.063.

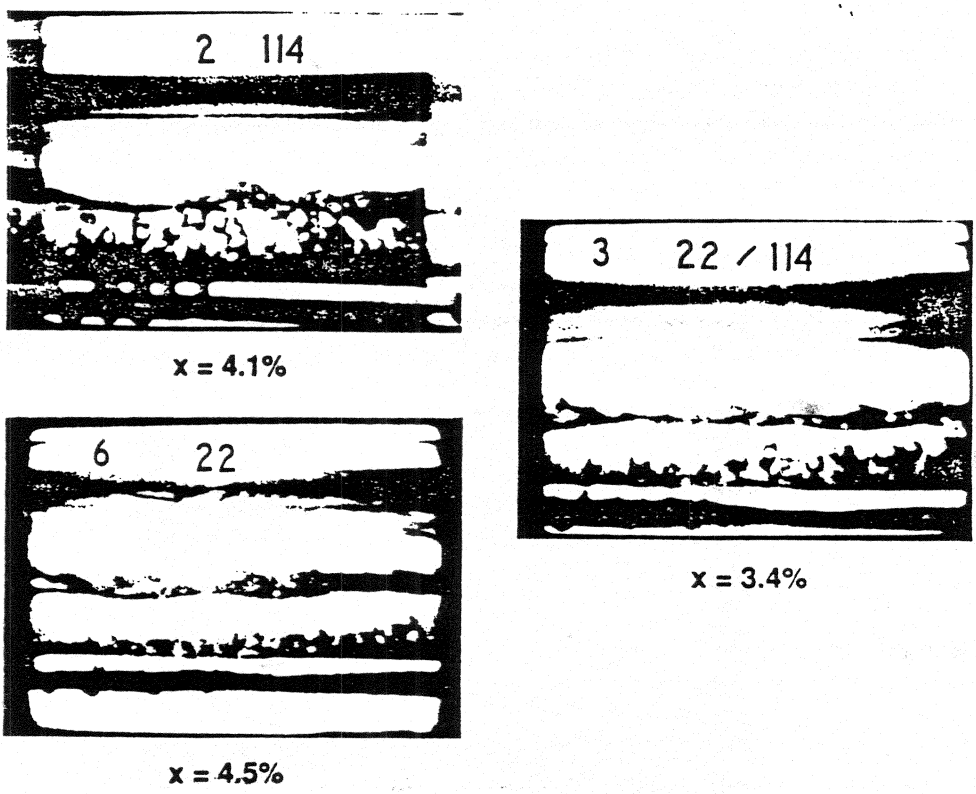

Fig. 10 Flow boiling for R114, R22, and a mixture for $x \approx 4\%$, $P_r = 0.063$.

total mass flow rate and fixed imposed heat flux. The lower Q_b is a result of higher vapor velocities, which reduce the thermal resistance to Q_c, thus removing superheat from the wall. Although the standard deviation is approximately 25% of the plotted Q_b, the Q_b is convincingly shown to decrease with increasing quality.

Figure 8 is a plot of the heat load required for nucleation of R114 at $q = 64$ kW/m^2 during flow boiling normalized by the heat load required for nucleation evaluated at $x = 0.012$ (Q_n) versus x. Data obtained from the films are plotted for two different sites. The data for these two sites agree well with each other, demonstrating the trend of decreased vapor generation with increased quality. The nucleate boiling portion of a flow boiling correlation by Gungor and Winterton [9] is plotted as a solid line on this graph. Gungor and Winterton modified Cooper's [10] pool boiling correlation with their own suppression factor to obtain an expression for the nucleate portion of a correlation for flow boiling within a horizontal tube. The nucleate portion of the correlation and data depart for the higher qualities. For example, the correlation predicts only a 23% reduction from the amount of nucleation at $x = 0.012$ to $x = 0.11$, where, as the data show, no bubbles are generated at $x = 0.11$ for the sites shown by filled and open circles.

The discrepancy between the data and Gungor and Winterton's correlation can be partially attributed to a difference in surface roughness between the quartz tube and what was assumed for the correlation. Gungor and Winterton [9] assumed that the surface

roughness of the tube was 1 μm. The surface roughness of the quartz tube was estimated from an electron microscope to be 0.5–0.2 μm. The smaller cavities of the quartz tube result in less heat transfer by bubble nucleation than what would be expected from a larger, 1-μm cavity. Another cause for the difference between the data and theory may be the inability of the Gungor and Winterton correlation to predict the suppression factor for the data. Their suppression factor is calculated from a simple and convenient correlation which relies on very few fluid properties. Consequently, it is understandable how the simple correlation for the suppression factor may not predict the suppression trends for the particular data set presented here.

R22, R114, and Mixture at P_r = 0.063

The remaining data will be examined solely by photographic evidence. Figures 9 through 13 are photographs taken with high-speed films of R114, R22, and the 37.7 mol% R22/62.3 mol% R114 mixture all at P_r = 0.061. Immediately, three general observations can be obtained from the figures. First, the number of bubbles present decreases as quality increases for all fluids studied. Second, for a given quality, R114 exhibits more bubbles than either R22 or the mixture. Third, the amount of nucleation by R22 and the mixture seems to be approximately the same. This is true even though the mixture is mostly R114 by mole. One might assume that the bubble activity ought to

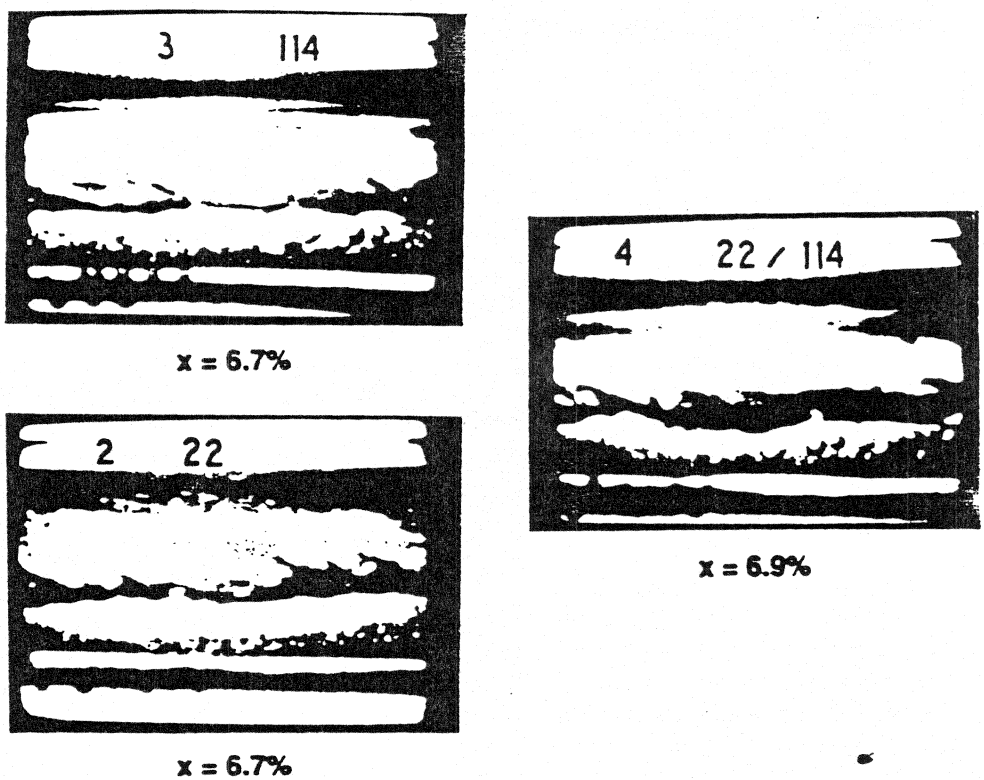

Fig. 11 Flow boiling for R114, R22, and a mixture for x = 7%, P_r = 0.063.

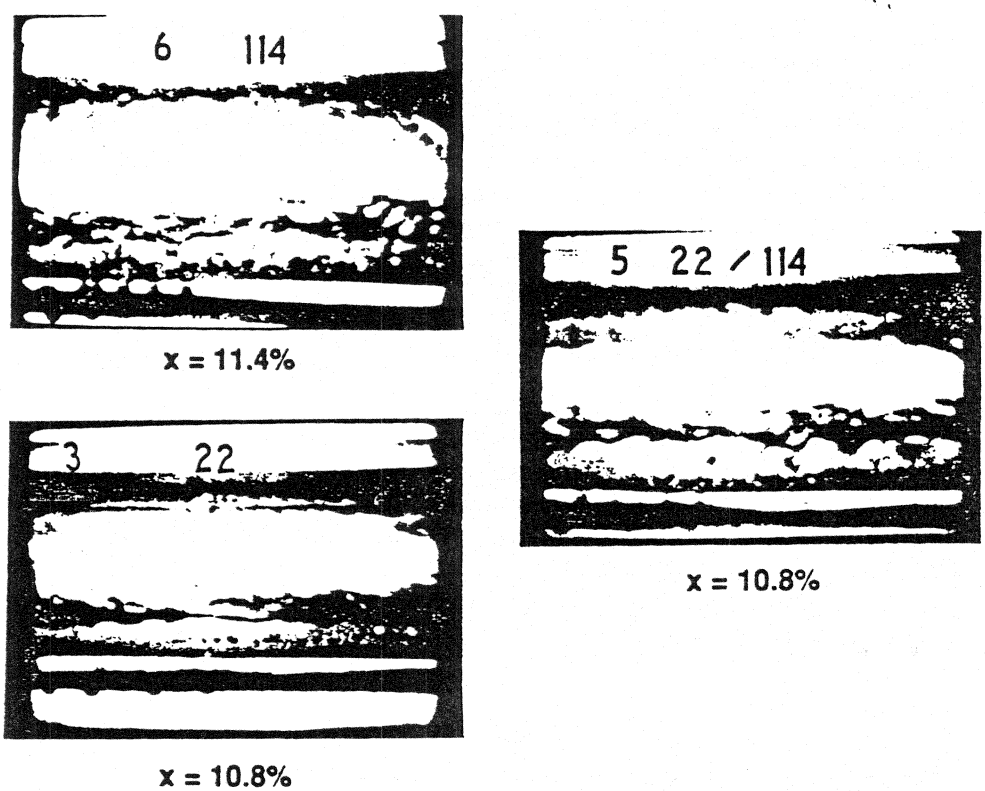

Fig. 12 Flow boiling for R114, R22, and a mixture for $x \approx 11\%$, $P_r = 0.063$.

be a mole-weighted activity where the resulting bubble activity would more closely resemble that of R114. The visual observations contradict this premise.

Table 1 shows the fluid properties at the test conditions for all the fluids tested. The last column of Table 1 represents the volume of vapor generated per joule of energy for a single bubble $[1/(\lambda\rho_v)]$. The volume of vapor can be equated with the activity of nucleation. Likewise, the per-unit energy can be equated to the constant electric heat flux incident the tube bottom. Hence, the last column of Table 1 shows that, for fixed heat flux, the predicted volume of vapor generated, or nucleate activity, for R22 differs by only 8% from that for the mixture, thus suggesting that the amount of nucleation for R22 should not differ much from the mixture. This is supported by the photographs in Figs. 10 through 12. Notice also that $1/(\lambda\rho_v)$ for R114 is 42% larger than $1/(\lambda\rho_v)$ for R22. The photographic evidence also supports this significant difference between the nucleate boiling for R114 and R22.

Another factor that determines the nucleate flow boiling activity of a liquid is its thermal conductivity (k_l). If it was possible to have a fluid that would become less thermally conductive for fixed flow and heat transfer conditions, it would be possible to observe a corresponding loss in bubble activity due to increased convection. Superheat is more readily convected from the wall for fluids with higher k_l. Consequently, nucleate flow boiling, in response to reduced wall superheat, will become less vigorous. The fifth column of Table 1 demonstrates the trend of liquids with lower thermal conductivity to

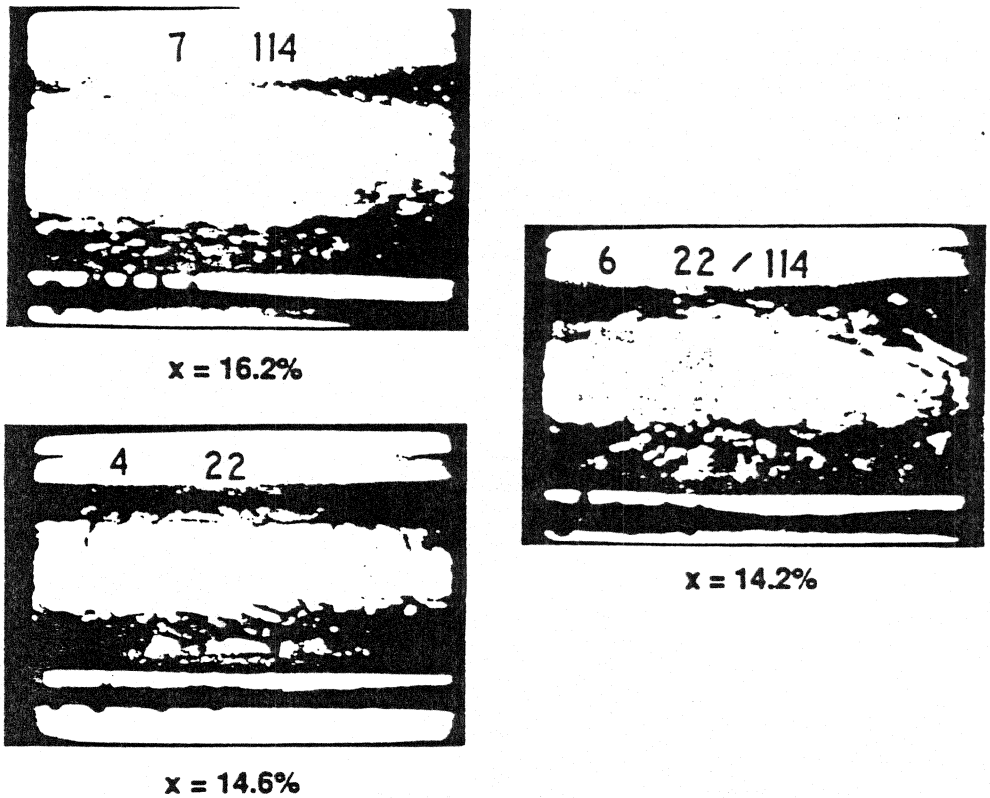

Fig. 13 Flow boiling for R114, R22, and a mixture for $x \approx 14.4\%$, $P_r = 0.063$.

exhibit more nucleate activity. For example, k_l of R114 is 41% lower than that for R22, which agrees with the result of this article, which indicate that the volume of vapor generated with R114 is greater than that of R22 for the same P_r. The thermal conductivity of the R114 is increased by 21% by the addition of R22 to obtain a 37.3 mol% mixture. The thermal conductivity of the liquid has been raised and the bubble activity correspondingly drops.

CONCLUSIONS

It has been demonstrated visually that a decrease in nucleate boiling during flow boiling is associated with an increase in quality for R114, R22, and a 37.7% R22/62.3%

Table 1 Fluid Properties at Test Conditions

Fluid	T_s (K)	P_s (kPa)	λ (J/kg)	k_l (W/m K)	g/mol	ρ_v (kg/m^3)	$1/\lambda\rho_v$ [(m^3/J) $\times 10^{-7}$]
R114	297	206	126.947	0.0647	170.92	15.95	4.94
R22	259	305	216.373	0.1068	86.47	13.31	3.47
R22/R114	271	265	160.834	0.0825	139.08	16.41	3.79

R114 mixture. The reduction in nucleate activity was demonstrated for the heat flux, total mass flow rate, and reduced pressure all fixed. Nucleation activity was shown to be also suppressed by a reduction in fluid pressure, which is in agreement with the trend of Cooper's [7] correlation for pool boiling on the outside of a horizontal cylinder. The films suggest that for a given quality, R114 exhibits much more nucleation than either R22 or the mixture. The amount of nucleation demonstrated by R22 and the mixture was comparable even though the mixture was mostly R114 by mole. Arguments using the latent heat of vaporization, the vapor density, and the liquid thermal conductivity have been made to explain the visual trends.

This study has shown that the parameters essential to obtaining the heat required for the growth and release of a bubble can be measured directly at low reduced pressure. However, there still remain some difficulties associated with the precision of the frequency measurement. Specifically, the measured bubble frequency had a large standard deviation and did not show a consistent tendency with quality. Further investigation is required to develop a method that can be used to produce statistically sound bubble frequency measurements. On the other hand, the bubble diameter was shown to be amiable to measurement by the high-speed-film technique as demonstrated by the low standard deviation of the measurement and consistent trends of the measurement with quality.

REFERENCES

1. D. Gorenflo, P. Blein, G. Herres, W. Rott, H. Schomann, and P. Sokol, Heat Transfer at Pool Boiling of Mixtures with R22 and R114, *Int. J. Refrig.*, vol. 11, pp. 257–263, July 1988.
2. T. O. Hui and J. R. Thome, A Study of Binary Mixture Boiling: Boiling Site Density and Subcooled Heat Transfer, *Int. J. Heat Mass Transfer*, vol. 28, no. 5, pp. 919–928, 1985.
3. K. Stephan, Heat Transfer in Boiling of Mixtures, *Proc. 7th Int. Heat Transfer Conf.*, Munich, paper RK14, pp. 59–81, 1982.
4. D. S. Jung, Mixture Effects on Horizontal Convective Boiling Heat Transfer, Ph.D. thesis, University of Maryland, College Park, MD, 1987.
5. J. G. Collier and D. J. Pulling, Heat Transfer to Two-Phase Gas-Liquid Systems, Part II: Further Data on Steam/Water Mixtures in the Liquid Dispersed Region in an Annulus, AERE-R 3809, 1962.
6. D. B. R. Kenning and G. F. Hewitt, Boiling Heat Transfer in the Annular Flow Regime, *8th IHTC*, San Francisco, pp. 2185–2190, 1986.
7. M. G. Cooper, Correlations for Nucleate Boiling—Formulation Using Reduced Properties, *PhysicoChem. Hydrodynam.*, vol. 3, no. 2, pp. 89–111, 1982.
8. G. Morrison and M. McLinden, Application of a Hard Sphere Equation of State to Refrigerants and Refrigerant Mixtures, NBS Technical Note 1226, Natl. Bur. Std., Gaithersburg, Md., 1986.
9. K. E. Gungor and R. H. S. Winterton, A General Correlation for Flow Boiling in Tubes and Annuli, *Int. J. Heat Mass Transfer*, vol. 29, no. 3, pp. 351–358, 1986.
10. M. G. Cooper, Saturation Nucleate Pool Boiling. A Simple Correlation, 1st U.K. Natl. Conf. Heat Transfer, vol. 2, *IChE Symp. Ser. No. 86*, pp. 785–793, 1984.